International Conference on Mechanical System Engineering and Technology Applications (ICoMSETA) 2024, pp. X – XX

ORIGINAL ARTICLE

OPTIMIZATION OF NOTCH HINGE DESIGN FOR ENHANCED PERFORMANCE IN ULTRASONIC VIBRATION-ASSISTED MACHINING

Azyufito Azra Nasution[1, a], Teddy Sjafrizal[1, b] and Rino Andias Anugraha[1, c]

[1]Industrial Engineering Department, School of Industrial Engineering, Telkom University, Bandung 40257, Indonesia

[a]Azyufito@student.telkomuniversity.ac.id, [b]teddysjafrizal@telkomuniversity.ac.id
[c]rinoandias@telkomuniversity.ac.id

Abstract. Ultrasonic vibration-assisted machining (UVAM) leverages intermittent cutting induced by a vibrated tool. The vibrations are often improved by employing flexure hinges to enhance the vibration transfer from actuator to the tooltip within the UVAM module. Notch hinges, among the various flexure hinge types, are the most widely employed hinges due to their proven capabilities and ease of manufacturing. This study employed finite element simulations to analyse the influence of notch hinge design parameters (radius, wall thickness, and hinge thickness) on hinge deformation and hinge stress. A full factorial design with five levels for each parameter was implemented. Larger notch radii increased hinge deformation, while thicker walls and hinges had the opposite effect. Induced stress remained minimally affected by hinge thickness but significantly decreased (≈ -30%) with larger radii. Grey relational analysis identified the optimal design combination in the current investigation as a notch with a 3 mm radius, 2 mm wall thickness, and 16 mm hinge thickness. This configuration achieved a simulated maximum hinge deformation of 1.95 μm and a stress of 64.3 MPa. These findings may contribute to a deeper understanding of notch hinge design for UVAM applications, potentially leading to wider adoption of this machining technique across various industries.
Keywords: Ultrasonic vibration-assisted machining, Flexure hinge, Notch hinge, Deformation, Finite element analysis

1. Introduction

Ultrasonic Vibration-Assisted Machining (UVAM) represents a significant advancement in conventional machining processes. Introduced in the late 1950s, UVAM has found applications across various machining processes and is particularly prevalent in precision manufacturing sectors such as aerospace, automotive, biomedical engineering, and ICT hardware [1]. UVAM was identified to be utilized in the component fabrication of Boeing B787 and Airbus A350, suggesting its critical role in these high-precision fields [2].

The superiority of UVAM in the cutting process is demonstrated through its intermittent cutting capability. This periodic engagement and disengagement between the tool and the workpiece are facilitated by the actuated vibrations from the vibrator module, as illustrated in Figure 1. This cutting approach significantly reduces average cutting forces by up to 50% compared to conventional machining

(CM) [3]. Additionally, UVAM achieves a superior average surface roughness by up to 50% compared to conventional machining, resulting in higher quality cutting outcomes [4]. This advanced machining mechanism notably extends the tool life. Conventional cutting processes using diamond tool on ferrous material typically caused about 9 µm of tool wear, whereas UVAM reduced this wear to just 3 µm [5]. The enhanced performance of UVAM can be attributed to its unique mechanism, which involves the integration of ultrasonic vibrations into the cutting process, generated by a high-frequency vibrator module that induces micro-scale oscillations in the tool.

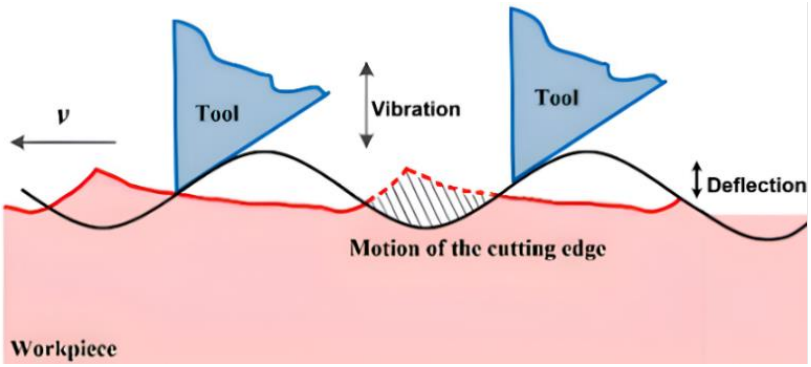

Figure 1. Cutting tool oscillation at given vibration frequency creating intermittent cutting, where v is the feed rate (mm/min), and the tool vibrates perpendicularly to the workpiece's long axis.

The oscillation is determined by the UVAM vibration module, which employs piezoelectric actuators to generate vibrations that affect the sinusoidal motion of the tool [6]. The piezoelectric actuators generate high-frequency, small-amplitude vibrations that facilitate the material removal process [7]. Previous studies have indicated that a significant removal rate is to be expected when vibrations are applied at an amplitude of more than 1 µm [8]. Nevertheless, the typical amplitude generated by the piezoelectric is approximately 0.001 µm [9], which is below the required level. Accordingly, the design of the UVAM vibration module presents a challenge in achieving the desired oscillating amplitude for the tool.

The alternative design of the recent non-resonant UVAM module employs flexure hinges to enhance the tool's vibration [10]. By Using flexure hinges, the deflection value in UVAM can be increased to more than 1 µm [11]. Incorporating flexure hinges can lead to an approximate 50% reduction in cutting force and a 30% improvement in surface finish quality when compared to UVAM setups without flexure hinges [12–14]. Flexure hinges are highly stretchable, resulting in significant deformation [15]. This characteristic makes them ideal for positioning close to the piezoelectric actuators, as their elastic properties can amplify the vibration with high deformation based on the force exerted by the actuator.

Flexure hinges can be varied in shape, with two main types of flexure hinge, namely Notch hinge and Leaf Spring Hinge. Unlike Leaf Spring Hinges, Notch hinges offer higher accuracy, better strength, and more concentrated deformation [16]. Furthermore, notch hinge also has strong bending and more flexible properties due to their semicircular shape, making them easier to fabricate and minimizing production costs [15]. A study by Gu Y [12], used notch hinge to allow flexibility in the vibration device for achieving precise and controlled motion, which is essential for the polishing process The advantages of notch hinges make them a highly versatile component, particularly in applications where vibration control is a key requirement.

As illustrated in Figure 2a, the force (F) actuated by the piezoelectric generates higher strain around the hinge, promoting larger deformation (w). This condition is highly dependent on the selected notch hinge design. Therefore, it is important to understand the effect of the design parameters on the deformability of this notch hinge in order to enhance its functionality in the context of a UVAM vibration module. Debongnie [17] proposes an equation

$$w = \frac{M_f}{E(b)} \frac{R^{3/2}}{t^{5/2}} \left[\frac{9\pi}{2} - 6\sqrt{\frac{t}{R}} \right] \quad (1)$$

to calculate the amount of hinge deformation as a function of its design parameters, where R is hinge radius, t is wall thickness and b is hinge thickness. This equation indicates that an increase in notch radius results in enhanced deformation, whereas an increase in wall and hinge thickness has the opposite effect, leading to a reduction in deformation. Empirically, the ratio between thickness and hinge radius has been shown to correlate with the resistance of the notch hinge to deformation [18]. However, designers of notched hinges must consider the increased stress around the hinge as the wall and hinge thickness is reduced.

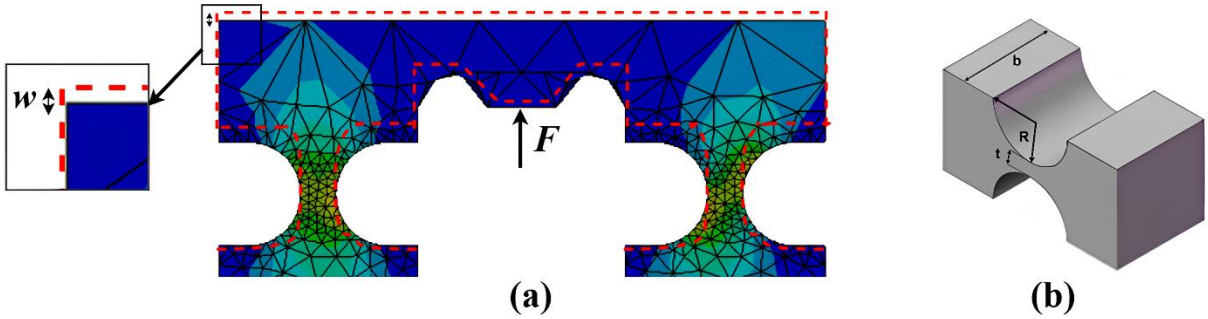

Figure 2. The vibration mechanism of the Notch hinge on force (F) and deformation (w), Flexure hinge stretches when applied force (a) and also one of the flexure hinge designs which is notch hinge with its parameters design (b), where R = radius (mm), t = wall thickness (mm), and b = hinge thickness (mm)

Despite the preceding findings regarding the impact of individual parameters on hinge deformation, the combined effect of notch hinge design parameters on maximum hinge deformation and minimum hinge stress remains unclear. This study aims to propose an optimal notch design capable of producing large deformation and supressed hinge stress.

2. Experimental setup

The study to propose an optimal notch hinge design for a UVAM application was performed through a series of finite element analysis (FEA). This objective was achieved by generating models using the full factorial method, which incorporated three design parameters, each with five levels (Table 1). A total of 125 model combinations were created and subsequently analysed using FEA in ANSYS Workbench 2021. The results from the FEA were utilized to determine the natural frequency, hinge deformation, and hinge stress for each model.

Table 1. Design parameters and their respective levels used in the simulation models of notch hinges.

Parameter	Level 1	Level 2	Level 3	Level 4	Level 5
Radius (R)	1 mm	1.5 mm	2 mm	2.5 mm	3 mm
Wall thickness (t)	2 mm	2.5 mm	3 mm	3.5 mm	4 mm
Hinge thickness (b)	16 mm	16.5 mm	17 mm	17.5 mm	18 mm

Prior to conducting the FEA simulation, the material and model setup steps were defined. The chosen material for the models was AISI 1040 (density= 7844.5 kg/m³, Young's modulus = 201.6 GPa, Poisson's ratio = 0.26, bulk modulus =140 GPa, and shear modulus = 80 GPa). AISI 1040 was selected for its favourable elastic properties and its machinability rating of 60 [19], which indicates relatively good machinability. The simulated model Figure 3b was derived through a simplification process of the

referenced UVAM vibration module. The RNO vibrator (Figure 3a) was chosen as the reference due to its promising performance reported in previous studies by Hakim, Lukman Nul [20].

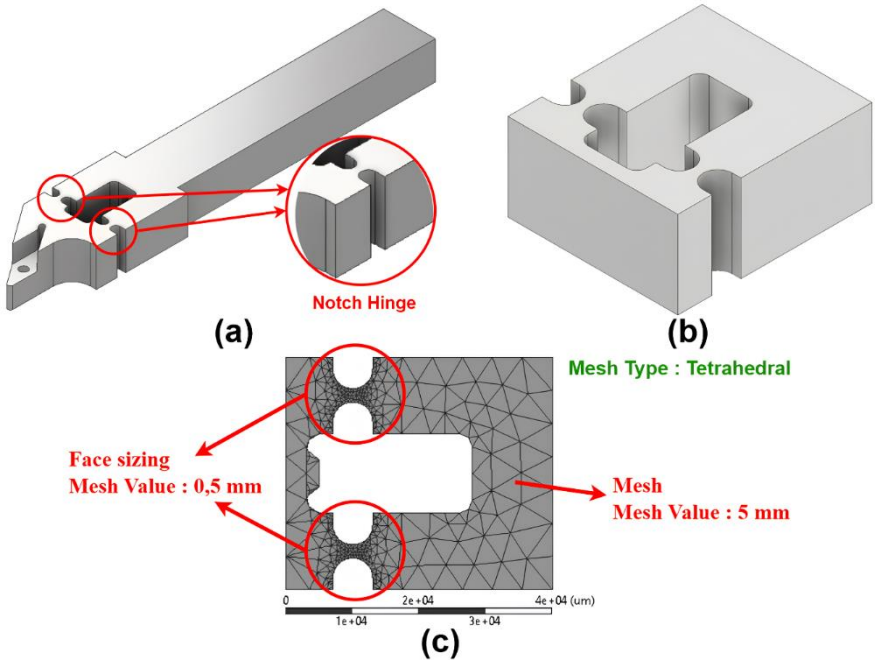

Figure 3. Where (a) is an existing Vibration tool with Notch hinge, (b) is a simplification model taken from the existing Notch hinge and (c) Mesh settings on software that focuses on Notch Hinge's capabilities with mesh size smaller than other planes

Following the material and model setup, modal analysis was conducted on each model to determine the natural frequency of the notch hinge design. Each model was constructed using a tetrahedral mesh with two distinct mesh sizes of 0.5 mm and 5 mm, respectively Figure 3c. A wide range of ultrasonic frequencies (18–30 kHz) was employed, encompassing three modal natural frequencies. Following the identification of the simulated natural frequencies for each model, 20 kHz was selected as it was distant from the simulated natural frequencies of all models Figure 4 and validated by harmonic response result in Figure 6 that the selected frequency caused low effect to the deformation. This frequency was then used for the subsequent performance analysis of the notch hinge.

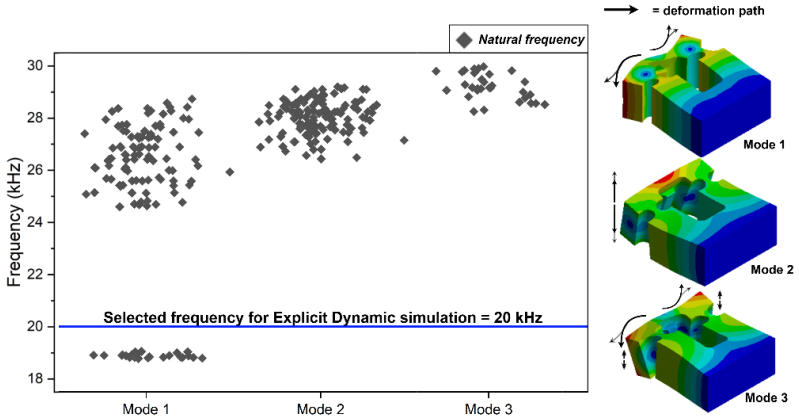

Figure 4. Distribution of the simulated natural frequencies of the models. The 20 kHz vibration is suitable for subsequent evaluation, given its considerable distance from the natural frequency range.

The characteristics of the notch hinge designs was assessed through the utilisation of explicit dynamic simulation. This method of FEA generated deformation and stress values of each simulation model. The mesh settings were identical to those employed in the preceding modal analysis. The capacity of each notch hinge to enhance actuated vibration of UVAM was optimised with consideration of a 3500 N force actuated from the piezo. This force was applying 5 times to replicate 5 vibrations. The cutting point on the model was loaded with a cutting force of F_x = 4.466 N, F_y = 139.024 N, and F_z = 80.282 N [21], mimicking the actual cutting condition. Subsequently, the optimised notch design, exhibiting both large deformation and reduced hinge stress, was selected following the completion of the grey relational analysis.

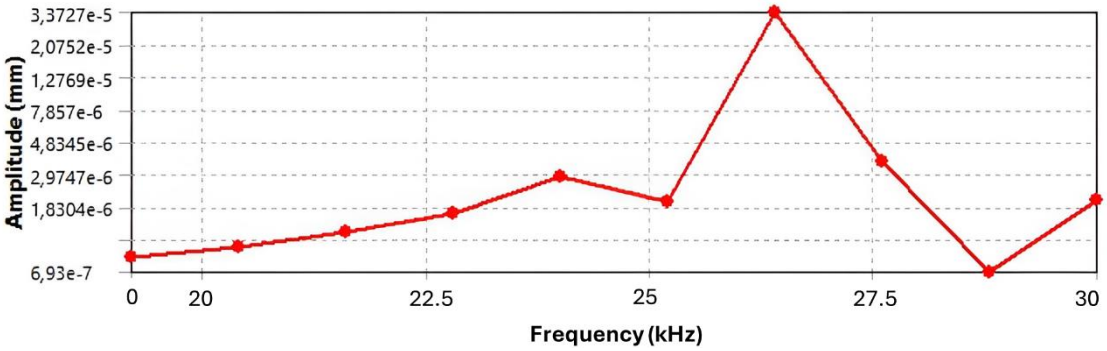

Figure 5. Harmonic response's result validated that the selected frequency (20 kHz) caused small effect to the notch hinge's deformation

3. Results and discussion

3.1 Effect of notch hinge design parameters on hinge deformation.

The impact of modifying the radius, wall thickness, and hinge thickness on hinge deformation and stress is illustrated in Figure 6. Deformation, which correlates with higher amplitude vibrations, is more pronounced when the wall thickness decreases and the hinge radius increases. Specifically, a reduction in wall thickness from 4 mm to 2 mm resulted in an increase in hinge deformation from 0.34 µm to 0.75 µm, more than doubling the deformation. However, reducing the hinge thickness from 18 mm to 16 mm resulted in a modest 13% increase in deformation. Similarly, a 20% improvement in deformation was achieved when the notch radius was increased from 1 mm to 3 mm.

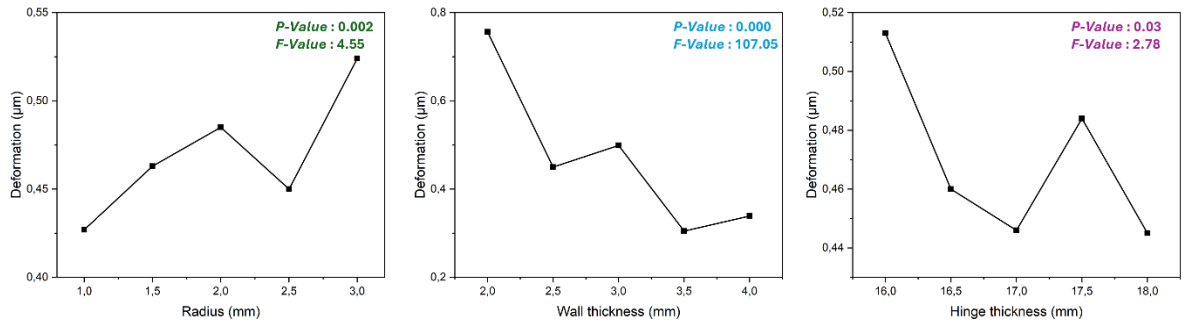

Figure 6. Deformation characteristics of notch hinge models simulated by finite element analysis. (a) Larger deformation observed with increased notch radius, and reduced deformation observed with increased (b) wall thickness and (c) hinge thickness.

These findings indicate that wall thickness is a critical parameter in influencing hinge deformation, with a significant reduction in thickness leading to a substantial increase in deformation. This suggests that for applications requiring high amplitude vibrations, optimizing wall thickness is essential. On the

other hand, changes in hinge thickness and notch radius, while still impactful, have a relatively lesser effect on deformation. The 13% improvement in deformation with a small reduction in hinge thickness implies that further reductions might yield diminishing returns, and thus, a balanced approach must be taken when adjusting this parameter. Similarly, the 20% improvement achieved by altering the notch radius highlights the importance of geometric considerations in the design process.

Comparing the simulated results gathered from the FEA simulations with the theoretical calculations suggested by Debongnie [17] is presented in Figure 7. Within the investigated range, the overall trend of changing radius, wall thickness, and hinge thickness on the normalized deformation of the hinge aligns with the theoretical calculations. This comparison validates both the FEA simulations and the theoretical models, demonstrating that they can be reliably used in designing notch hinges for UVAM applications especially in predicting the deformation characteristics.

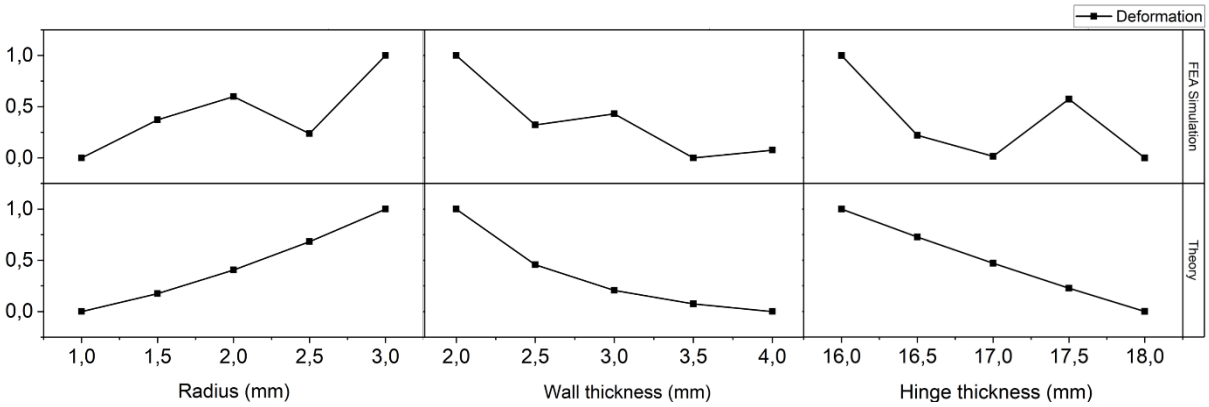

Figure 7. The global trend of hinge deformation simulated by finite element analysis aligns with the calculation proposed by Debongnie et al. [17].

3.2 Effect of notch hinge design parameters on hinge stress

Having a highly flexible notch hinge comes with the challenge of increased stress in the vicinity of the hinge. Therefore, after enhancing the deformation capability of the hinge, the investigation was extended to identify the stress experienced on each model. The simulated hinge stresses, determined by FEA as functions of radius, wall thickness, and hinge thickness, are presented in Figure 8.

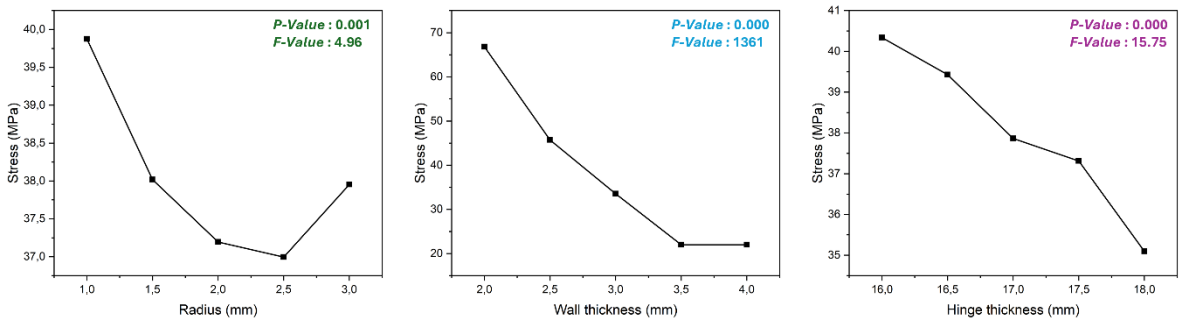

Figure 8. Hinge stress characteristics of notch hinge models simulated by finite element analysis. (a) Lower hinge stress could be realized with increased notch radius, thicker (b) wall thickness and (c) hinge thickness.

This study demonstrates that lower stress can be achieved with a larger radius, thicker walls, and increased hinge thickness. Among these three design parameters, increasing wall thickness had the most significant impact on reducing hinge stress. Specifically, doubling the wall thickness from 2 mm to 4

mm resulted in a 50% reduction in hinge stress. Similarly, increasing the hinge thickness by an additional 2 mm (from 16 to 18 mm) led to a 12% decrease in the stress exerted on the hinge.

Interestingly, the hinge with a radius of 3 mm exhibited a non-linear response in hinge stress. While initially reducing stress, the stress levels began to increase once the radius was flattened at 2.5 mm. This suggests that there is an optimal radius beyond which further increases may not provide additional benefits and could potentially lead to higher stress levels.

These findings highlight the importance of a balanced approach in optimizing notch hinge design parameters. Given the differing influences of each parameter on hinge deformation capabilities and stress reduction, identifying an optimal set of design parameters is crucial. Such optimization is expected to streamline the design process for notch hinges in UVAM applications, facilitating the creation of hinges that achieve the desired balance between flexibility and durability.

3.3 Finding optimal notch hinge design for UVAM applications

The grey relational analysis method was employed to identify the optimal notch hinge design, aiming to maximize hinge deformation (larger is better) and minimize hinge stress (smaller is better). The results are presented in Table 2. The optimized model, which was ranked first, features a radius of 3 mm, a wall thickness of 2 mm, and a hinge thickness of 16 mm. This model produced vibrations with an amplitude of 1.95 μm and a hinge stress value of 64.3 MPa.

Table 2. Ranking of the simulated models using grey relational analysis. The top-ranked model demonstrates optimized performance, exhibiting large hinge deformation and minimal stress.

Rank	R	t	b	D $x_i(k)$	S $x_i(k)$	D Δ_i	S Δ_i	D $\gamma_i(k)$	S $\gamma_i(k)$	γ_i
1	3	2	16	1.000	0.320	0.000	0.680	1.000	0.424	0.712
2	1	4	18	0.380	0.983	0.620	0.017	0.446	0.966	0.706
3	1.5	3,5	18	0.195	1.000	0.805	0.000	0.383	1.000	0.692
4	2	2	17	0.968	0.351	0.032	0.649	0.939	0.435	0.687
5	2	4	18	0.210	0.986	0.790	0.014	0.388	0.974	0.681
6	3	4	18	0.477	0.927	0.523	0.073	0.489	0.872	0.680
7	1.5	3,5	17,5	0.110	0.988	0.890	0.012	0.360	0.977	0.669
8	1	4	16	0.325	0.950	0.675	0.050	0.426	0.910	0.668
9	2	3,5	18	0.242	0.966	0.758	0.034	0.398	0.937	0.667
10	2,5	4	18	0.188	0.975	0.812	0.025	0.381	0.952	0.666

R = radius (mm), t = wall thickness (mm), b = Hinge thickness (mm), D = Deformation, S = Stress, $x_i(k)$ = normalization value, Δ_i = deviation sequence value, γ_i (k) = grey relational coefficient

Comparing this optimized model to the UVAM vibration module without a flexure hinge reveals a substantial increase in vibration amplitude (see Figure 9). The optimized notch hinge design resulted in a tenfold increase in the vibration module's amplitude compared to the module without the notch hinge. Nevertheless, concerns pertaining to the built-up hinge stress warrant further investigation. The simulated stress for this optimised design was 64 MPa, which is markedly lower than the tensile strength of AISI 1040 (620 MPa). This suggests that the notch hinge design exerts minimal influence on the structural integrity of the UVAM module. Ultimately, the substantial increase in vibration amplitude demonstrates the effectiveness of the optimized notch hinge in significantly enhancing the vibrational performance of the UVAM vibration module, while maintaining structural integrity and reliability

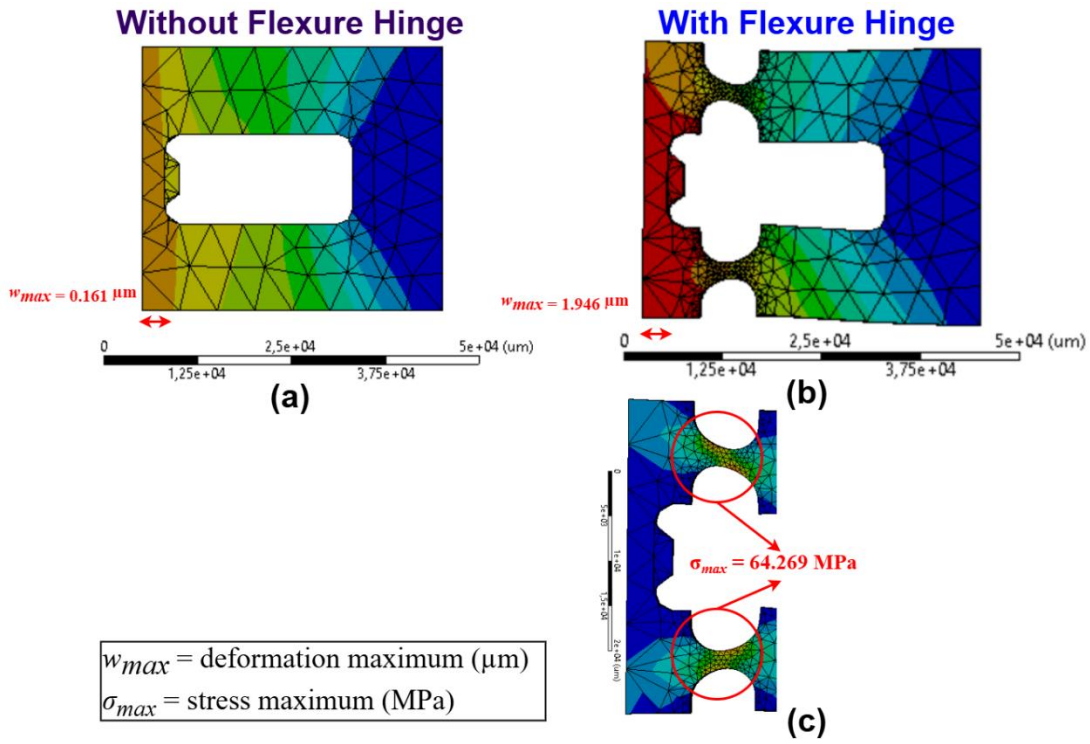

Figure 9. The UVAM vibration model with notch hinge exhibits larger hinge deformation (1.95µm) than the one without hinge (0.16 µm). (c) The notch hinged experiences relative low hinge stress (64.3 MPa), highlighting the superiority of the UVAM vibration module when equipped with notch hinge.

4. Conclusion

This study successfully identified optimized notch hinge design parameters for use in UVAM vibration modules by analyzing data gathered from finite element analysis (FEA) of various models. The findings demonstrate that notch hinge characteristics are highly dependent on three key design parameters: hinge radius, wall thickness, and hinge thickness. Within the investigated range, the optimal combination of these parameters to maximize deformation while minimizing stress was identified as a radius of 3 mm, a wall thickness of 2 mm, and a hinge thickness of 18 mm. This optimized hinge model can produce deformation values ranging between 0.969 and 1.946 µm. By achieving an optimized notch hinge design, UVAM vibration modules can operate with larger oscillation amplitude. The ability to maximize deformation while minimizing stress ensures that these modules can perform at higher levels without compromising structural integrity.

References

[1] Zheng L, Chen W, Huo D. Review of vibration devices for vibration-assisted machining. International Journal of Advanced Manufacturing Technology 2020;108:1631–51. https://doi.org/10.1007/s00170-020-05483-8.

[2] Gupta K, Pramanik A. ADVANCED MACHINING AND FINISHING. 2021.

[3] Shanker Dixit U, Mohan Pandey P, Chandra Verma G. Ultrasonic-assisted machining processes: a review. vol. 12. 2019.

[4] Gao Y, Sun R, Leopold J. Analysis of cutting stability in vibration assisted machining using an analytical predictive force model. Procedia CIRP, vol. 31, Elsevier B.V.; 2015, p. 515–20. https://doi.org/10.1016/j.procir.2015.03.014.

[5] Brehl DE, Dow TA. Review of vibration-assisted machining. Precis Eng 2008;32:153–72. https://doi.org/10.1016/j.precisioneng.2007.08.003.

[6] Kurniawan R, Ko TJ. A study of surface texturing using piezoelectric tool holder actuator on conventional CNC turning. International Journal of Precision Engineering and Manufacturing 2013;14:199–206. https://doi.org/10.1007/s12541-013-0028-8.
[7] Chen W, Huo D, Shi Y, Hale JM. State-of-the-art review on vibration-assisted milling: principle, system design, and application. International Journal of Advanced Manufacturing Technology 2018;97:2033–49. https://doi.org/10.1007/s00170-018-2073-z.
[8] Kurniawan R, Ko TJ, Han PW, Xu M, Chen J, Kwak YI, et al. FE simulation, analytical prediction, and experimentation of cutting force in longitudinal vibration-assisted milling (LVAM) during Ti-6Al-4 V cutting. International Journal of Advanced Manufacturing Technology 2023;126:1417–51. https://doi.org/10.1007/s00170-023-11092-y.
[9] Li G, Wang B, Xue J, Qu D, Zhang P. Development of vibration-assisted micro-milling device and effect of vibration parameters on surface quality and exit-burr. Proc Inst Mech Eng B J Eng Manuf 2019;233:1723–9. https://doi.org/10.1177/0954405418774592.
[10] Zheng L, Chen W, Huo D. Review of vibration devices for vibration-assisted machining. International Journal of Advanced Manufacturing Technology 2020;108:1631–51. https://doi.org/10.1007/s00170-020-05483-8.
[11] Yang Y, Wen J, Zhang Y. Development of a novel XZ workpiece vibration generator for cooperative vibration cutting of hierarchical grating structures. Mech Syst Signal Process 2023;198:110422. https://doi.org/10.1016/J.YMSSP.2023.110422.
[12] Gu Y, Zhou Y, Lin J, Lu M, Zhang C, Chen X. Design, analysis, and testing of a flexure-based vibration-assisted polishing device. AIP Adv 2018;8. https://doi.org/10.1063/1.5025498.
[13] Xu WX, Zhang LC. Ultrasonic vibration-assisted machining: principle, design and application. Adv Manuf 2015;3:173–92. https://doi.org/10.1007/s40436-015-0115-4.
[14] Júnior MG, França TV, Fortulan CA, da Silva RHL, Foschini CR. Green ceramic machining benefits through ultrasonic-assisted turning: an experimental investigation. International Journal of Advanced Manufacturing Technology 2022;118:3091–104. https://doi.org/10.1007/s00170-021-08174-0.
[15] Smith ST. Foundations of ultra-precision mechanism design 2003.
[16] Wu J, Zhang Y, Cai S, Cui J. Modeling and analysis of conical-shaped notch flexure hinges based on NURBS. Mech Mach Theory 2018;128:560–8. https://doi.org/10.1016/j.mechmachtheory.2018.07.005.
[17] Debongnie J-F, Raucent B, Merken P, Smal O, Debongnie JF, Raucent B. Design and test of a circular notch hinge. 2004.
[18] Yong YK, Lu TF, Handley DC. Review of circular flexure hinge design equations and derivation of empirical formulations. Precis Eng 2008;32:63–70. https://doi.org/10.1016/j.precisioneng.2007.05.002.
[19] Davey R. AISI 1040 Carbon Steel (UNS G10400). Https://WwwAzomCom/ArticleAspx?ArticleID=6525 2012.
[20] Lukman Nul Hakim, Rino Andias Anugraha, Teddy Sjafrizal, Nopendri, Pratya Poeri Suryadhinia, Mohd Rasidi Ibrahim. Effect Of Ultrasonically Vibrated Cutting Tool on Surface Roughness of Micro Turning. Journal of Advanced Research in Micro and Nano Engieering 2024;20:35–43. https://doi.org/10.37934/armne.20.1.3543.
[21] Yang L, Zhang M. Research on the Influence of Cutting Speed on Vibration Cutting Force. 2017.

Acknowledgments
This work is supported by Telkom University (*Penelitian Dana Internal Periode* 2-2023)